General Processing Approach for Bistatic SAR Systems: Description and Performance Analysis

Marc Rodriguez-Cassola, Pau Prats, Paco López-Dekker, Gerhard Krieger, Alberto Moreira
Microwaves and Radar Institute, German Aerospace Center (DLR), 82234 Wessling, Germany

Abstract

For its intrinsic properties, bistatic SAR processing cannot be approached in the same manner monostatic SAR processing is approached. In general, a bistatic SAR processor is more than a powerful focussing algorithm. Because of the lack of precise time (range) and phase (Doppler) references in non-cooperative (and even cooperative) bistatic systems, a prior software synchronisation step is used to correct the residual errors caused by the use of different clocks. Moreover, depending on the bistatic configuration, different kinds of SAR focussing algorithms can be used. Azimuth-invariant configurations may benefit from the convolution property of the Fourier transform, whereas more general configurations are better suited for efficient time-domain techniques. A discussion on the performance of three Fourier-domain focussing algorithms, range-Doppler, chirp scaling, and range migration, is included in the paper.

1 Introduction

Bistatic SAR processing, like regular monostatic, can be performed at very different levels, ranging from coarse to accurate filter strategies. However, the increase in the demand of accurate microwave remote sensing data requires the use of almost high-quality user-transparent imaging techniques. Since generalised bistatic SAR is not necessarily a synchronised system, a generalised bistatic SAR processor must consist of a previous synchronisation step followed by a bistatic SAR focussing kernel. In the general case, the bistatic SAR is also a non-cooperative system, thus the development of automatic processing approaches for the synchronisation of bistatic SAR data is a fundamental issue in the recent literature [1]-[3]. Moreover, due to the particularities of bistatic acquisitions, not any SAR focussing kernel is suitable to accurately focus bistatic SAR data. Depending on the symmetry of the acquisition frequency- or time-domain approaches are suggested.

The paper is structured as follows: Section 2 shows the block diagram of a generalised bistatic SAR processor; Section 3 discusses two different approaches for automatic synchronisation of bistatic SAR data, including an accuracy analysis; Section 4 includes a discussion on different approaches for efficient bistatic SAR focussing depending on the configuration, and also including a performance analysis for an exemplary configuration; Section 5 concludes the paper with a summary.

2 Bistatic SAR processing approach

Fig. 1 shows the block diagram of a general bistatic SAR processing chain; it can be seen that any *a priori* information on the clock error is introduced in the range/Doppler synchronisation stage. After this, a SAR focussing is performed, as complex as it might be depending on the bistatic acquisition. Using the focussed bistatic image, and depending on the amount of additional information available, the residual differential clock error can be estimated accordingly and reinjected on the first synchronisation stage. Then SAR focussing can be performed again, but this time using better synchronised bistatic raw data. The same procedure can be performed iteratively until the residual phase errors are kept under a tolerable level or no further improvement occurs. In the case of non-cooperative systems, there is clearly no differential clock information at the first synchronisation pass and it could thus only be performed in subsequent iteration steps.

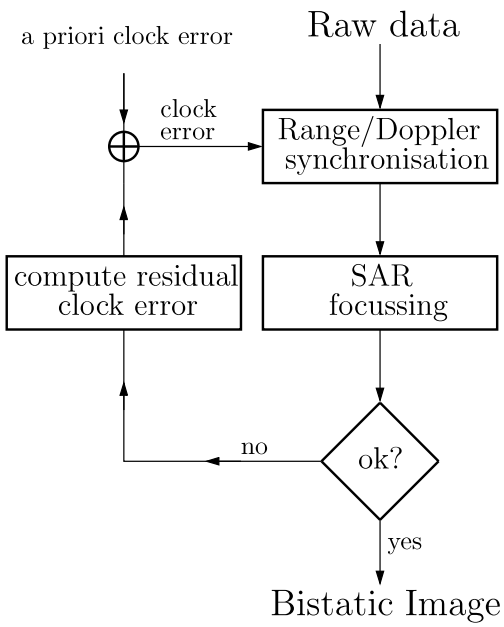

Figure 1: Block diagram of a generalised bistatic SAR processor.

3 Automatic synchronisation

The effect of using different clocks in a bistatic SAR causes a two-dimensional phase error in the bistatic data, which, if not corrected, has a direct impact on the focussing and phase quality of the acquired images [4]. Fig. 2 shows the effect of a realistic clock phase error on the phase of a bistatic image. The top plots show the phase (left) and frequency (right) clock errors, whereas the bottom plots show the coherence (left) and interferogram (right) computed using the bistatic image before and after synchronisation.

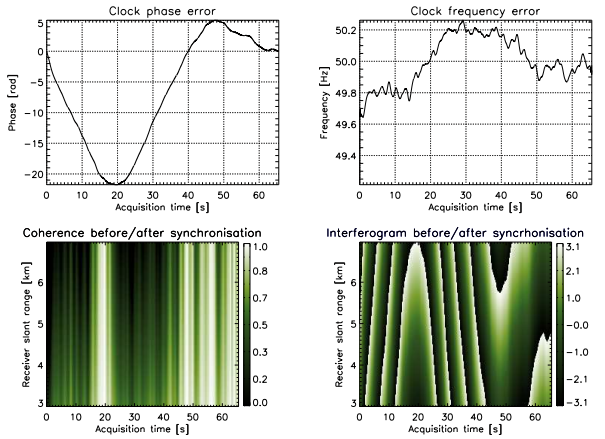

Figure 2: Effect of clock errors on bistatic image. Phase (top left) and frequency (top right) clock error. Coherence (bottom left) and interferogram (bottom right) computed with the bistatic image before/after synchronisation.

Unfortunately, differential clock errors are not necessarily the only source of residual phase errors in usual bistatic SAR systems. They are, however, the only genuinely bistatic phase error source, but which only add to the already well-known monostatic sources (residual motion errors, moving targets, atmospheric errors, etc.). The automatic synchronisation of the bistatic SAR data is carried out by estimating the residual clock error from the received data. Depending on the characteristics of the bistatic acquisition, a realistic model for the residual phase errors within the image has to be established. Measuring several realisations of this residual phase error functions (at least as many as unknowns our model has so that it is potentially invertible), the clock error might be inverted, then corrected, yielding better synchronised bistatic data. The quality of the estimate, as expected, strongly depends on the quality and quantity of residual phase error measurements available on the image.

3.1 Absolute phase error estimation

The absolute phase error estimation is performed using a single bistatic image. If the phase error can be at all estimated, then its correction yields a better focussed bistatic image. Thus, if only one single bistatic image is available, the only way of synchronising the bistatic raw data set is using an autofocus algorithm. Autofocus algorithms rely on the presence in the image of bright coherent targets, and therefore synchronisation might be difficult to achieve if a homogeneous scene is being imaged. If a model-based approach is selected (i.e., contrast maximisation, map drift, etc.) the estimation should be performed on subimages in order to retrieve, if possible, a two dimensional estimate of the residual phase errors. This kind of algorithms have a limited precision and are not able to estimate the absolute phase error within the image. If a point-like dependent algorithm like phase gradient is used, a better precision in the estimation can be expected, and under certain conditions (perfectly calibrated targets), the absolute clock error is potentially invertible; in any case the frequency offset is observable. The approach based on the estimation of the residual phase error using point-like targets on the image (i.e., phase gradient) is preferred due to its intrinsic precision. However, the quality of the phase error estimate depends on three essential points: a) the presence of enough point targets in the image, b) our ability to detect them successfully, and c) the SCR of the image. The accuracy of the measure can be approximated by

$$\sigma_\phi \approx \frac{1}{\sqrt{2 \cdot \mathrm{SCR} \cdot N}} \cdot \left(1 + \sqrt{\frac{5}{12 \cdot \mathrm{SCR}}}\right) \quad , \qquad (1)$$

where N is the number of points where the phase error measure is done. The assumption of large SCR is included in the derivation of (1) [5]. Fig. 3 shows the accuracy of the absolute phase error estimation as a function of the SCR and the number of control points within the image.

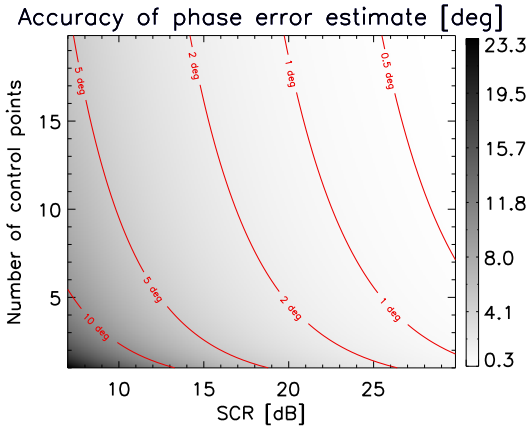

Figure 3: Accuracy of the absolute phase error estimation as a function of the SCR and number of phase error measures.

3.2 Differential phase error estimation

For a differential phase error estimation, a reference error-free image, together with the non-synchronised bistatic one, is needed. By measuring the azimuth coregistration

errors between both images, an estimate of the clock frequency error can be obtained. This method is a standard procedure in the estimation of residual phase errors for repeat-pass airborne interferometric applications, and has been already applied to the synchronisation of cross-platform bistatic airborne images [1]. However, there are two essential differences between the case discussed here and [1], both related to the fact that the residual phase error of the bistatic image is computed directly using the interferometric phase of the images: a) the validity of [1] requires coherence overlap between the bistatic and the reference image, and b) the estimation of the residual phase error is strongly affected by an error in the expected interferometric phase, i.e., errors in the DEM. High SNR or coherence between the images is not required, but improves the quality of the estimation. A first difference with respect to the absolute phase error estimation is revealed by the fact that an integration step is required to retrieve the phase error, thus not providing any information on the constant term of the phase error, just like in the absolute estimation performed on non-calibrated images. However, if both images are coherent, then the phase information of the reference image can be compared to the phase information of the bistatic image. After removing the offset introduced by any across-track baseline, the differential phase error, including the constant term, can be extracted from the interferogram between both images. The advantages and disadvantages of this method when compared to the autofocus approach are clear. On one hand, not only point-like, but also extended, and even distributed targets if both images are coherent, can be used for the phase error estimate, thus improving quality and robustness. On the other hand, the quality of the estimate is a function of the quality of the focussing of the master image, since the slave is only differentially corrected. Therefore, this method does not necessarily improve the quality of the slave image, but it definitely makes it more alike to the master reference. Note that, even if focussing improvement cannot be guaranteed, this differential correction can be very helpful to extract the interferometric information of the image pair, as has been presented in the results of the bistatic cross-platform interferometric pair of the DLR-ONERA airborne experiment [1].

Analogously to the results of Subsection 3.1, the final accuracy of the clock phase error can be expressed as

$$\sigma_\phi \approx \frac{4\pi}{\lambda \cdot \sum_i a_2^{-2}(r_i)} \cdot \sqrt{t_a} \cdot \sigma_t \quad , \qquad (2)$$

where λ is the radar wavelength, a_2 is the quadratic component of the bistatic range history, t_a is the azimuth time, and σ_t is the accuracy in the measure of the azimuth coregistration offset. This accuracy depends on the similarity between the reference image and the bistatic image, being of course improved if there is coherence between the images. A consequence of the differential measure is that the errors in the derivative propagate during integration steps, thus increasing the variance of the estimator for long image sizes -the term $\sqrt{t_a}$ in (2)-. In fact, accuracy worsens for arbitrarily long data takes, a clear drawback of the method. Fig. 4 shows the accuracy as a function of the coherence and the duration of the acquisition for the case of a bistatic along-track airborne acquisition like in the DLR-ONERA bistatic airborne experiment [1].

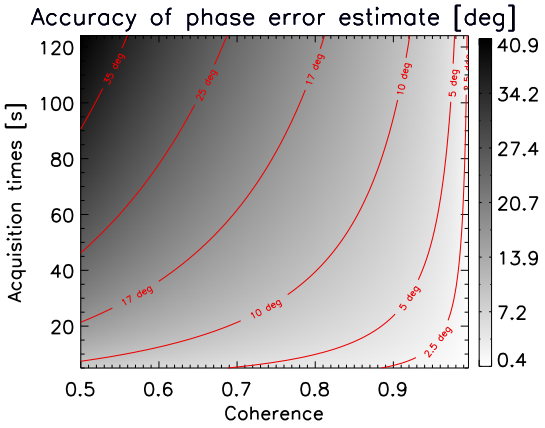

Figure 4: Accuracy of the differential phase error estimation as a function of coherence and of the acquisition time for an airborne bistatic along-track configuration of the DLR-ONERA experiment [1]. The accuracy of the coregistration offsets measure is assumed to be the Crámer-Rao bound for complex cross-correlation. Non-weighted LMS approach.

4 Efficient bistatic SAR focussing

When considering the focussing approach most appropriate for the case, bistatic SAR acquisitions can be divided into two main categories: a) azimuth-invariant and b) azimuth-variant. The linear and parallel tracks, and constant and equal speed case shares the azimuth-invariance property of monostatic SAR, whereas any more general configurations show an azimuth-variant character. In order to profit of the convolution property of the Fourier transform, azimuth-invariant configurations are particularly suited for frequency-domain focussing techniques, like range-Doppler (RD), chirp scaling (CS) or range migration (ωK) algorithms. These algorithms have been frequently addressed in the bistatic SAR imaging literature as capable of focussing azimuth-variant configurations, but only in an approximate manner. Moreover, the fact that bistatic SAR focussing is a fully 3D task introduces a further drawback for this kind of techniques: the accuracy of the algorithm depends, not only on the intrinsic approximations of the algorithm, but also on the imaged scene. Azimuth-variance, on the contrary, is difficult to accommodate in an accurate manner using frequency-

domain algorithms, and therefore a time-domain approach is preferred. Due to the complexity of simultaneously achieving precise bistatic imaging and small computational load using frequency-domain techniques, a new processing algorithm based on fast factorised backprojection (FFBP) [6] has been developed [7], [8]. The new imaging algorithm, named bistatic fast factorised backprojection (BFFBP), achieves precise accommodation of azimuth-variance and topography of general bistatic SAR acquisitions, while keeping a speed-up factor proportional to $\log_2 N$ with respect to direct backprojection (DBP), in a similar manner as frequency-domain algorithms do. BFFBP has the advantage of working on a bounded-error basis, where the amount of error is controllable with the quality of the involved interpolators [7]: the more precise, the slower the algorithm. As a rule of thumb, high-quality BFFBP is usually less-than-one-order of magnitude slower than its frequency-domain counterparts, and therefore these may be preferred for the focussing of data of bistatic azimuth-invariant configurations. In general, RD and CS are equivalent approaches, capable of accommodating the non-hyperbolical range histories but showing the typical shortcomings of the algorithms for monostatic SAR: poor wide-swath/wide-bandwidth performance. ωK improves the performance of RD and CS, but loses its fundamental advantage of monostatic SAR: inversion exactness. Higher bandwidths and swaths can be focussed using ωK but the algorithm behaviour is analogous to that of RD and CS. Bistatic ωK shares with its monostatic version its hostility to the inclusion of space-variant 2D corrections, essential in the bistatic case for topography accommodation. Since BFFBP delivers an arbitrarily low error image, only the performance of the frequency-domain algorithms for the bistatic configuration of Table 1 is presented.

Table 1: Simulation parameters for reference airborne configuration

Tx reference height [m]	1500
Along-track baseline [m]	100
Across-track horizontal baseline [m]	2000
Across-track vertical baseline [m]	10
Platforms velocity [m/s]	90
Transmitted bandwidth [MHz]	100

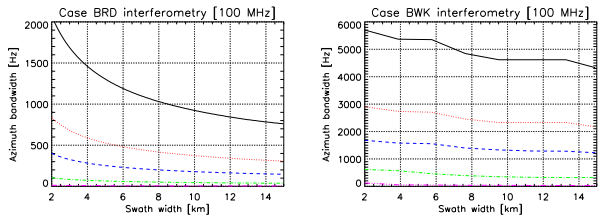

Figure 5: Maximum azimuth bandwidths which can be processed using RD/CS (left) and ωK (right) for the reference airborne acquisition of Table 1. Results for X-band (solid), C-band (dotted), S-band (dashed), L-band (dashed-dotted), and P-band (dashed-3dotted). Curves correspond to a phase error on the maximum of the impulse response smaller than 5°.

Fig. 5 shows the maximum azimuth bandwidth as a function of the swath width which can be processed using RD/CS (left) or ωK (right) so that the phase error at the maximum of the impulse response is lower than 5° for different radar frequencies, X, C, S, L, and P band. ωK has a decreasing performance for increasing swath widths too, as it can be seen in Fig. 5. Results are scalable with the transmitted chirp bandwidth: using 300 MHz instead of 100 MHz would make the values on the plots reduce by a factor 9.

5 Summary

A generalised approach for high-precision bistatic SAR processing has been presented in the paper. The processing includes an automatic synchronisation part and an efficient and precise SAR focussing kernel. Processing is understood in an iterative manner, and updates of the residual clock phase error are computed after every new processing step. A simplified performance analysis of the automatic synchronisation approaches and of the frequency-domain SAR focussing algorithms has been included in the paper.

References

[1] H. Cantalloube *et* al, *Challenges in SAR processing for airborne bistatic acquisitions*, Proc. EUSAR 2004, pp. 577-580, Ulm, Germany.

[2] P. López-Dekker *et* al, 'Phase Synchronization and Doppler Centroid Estimation in Fixed Receiver Bistatic SAR Systems', *IEEE Trans. Geosci. Remote Sens.*, vol. 46, no. 11, pp. 3459-3471, Nov. 2008.

[3] M. Rodriguez-Cassola *et* al, 'Bistatic TerraSAR-X/F-SAR spaceborne-airborne SAR experiment: description, data processing and results', *IEEE Trans. Geosci. Remote Sens.*, vol. 48, no. 2, pp. 781-794, Feb. 2010.

[4] G. Krieger *et* al, 'Impact of oscillator noise in bistatic and multistatic SAR', *IEEE Geosci. Remote Sens. Lett.*, vol. 3, no. 3, pp. 424-428, Jul. 2006.

[5] W. Ye *et* al, 'Weighted Least-Squares Estimation of Phase Errors for SAR/ISAR Autofocus', *IEEE Trans. Geosci. Remote Sens.*, vol. 37, no. 5, pp. 2487-2494, Sep. 1999.

[6] L. Ulander *et* al, 'Synthetic-aperture radar processing using fast factorized back-projection', *IEEE Trans. Aerosp. Electr Syst.*, vol. 39, no. 3, pp. 760-776, Jul. 2003.

[7] M. Rodriguez-Cassola *et* al, 'Efficient Time-Domain Image Formation with Precise Topography Accommodation for General Bistatic SAR Configurations', submitted to *IEEE Trans. Aeros. Electr. Syst.*

[8] M. Rodriguez-Cassola *et* al, *Efficient Time-Domain Focussing for General Bistatic SAR Configurations: Bistatic Fast Factorised Backprojection*, Proc. EUSAR 2010, Aachen, Germany.